Theor. Appl. Climatol. 63, 149–161 (1999)

Theoretical and Applied Climatology

School of Geography and Environmental Studies, University of Tasmania, Australia

Cloud Transmission Estimates of UV-B Erythemal Irradiance

C. Kuchinke and **M. Nunez**

With 7 Figures

Received January 4, 1998

Summary

Two UV-Biometer 501A instruments were used to estimate global erythemal irradiance at two locations in southwest Sweden; the Earth Sciences Centre, University of Göteborg (57.69° N; 11.92° E) and the island of Nordkoster, 200 km to the north (58.83° N; 10.72° E).

A semi-empirical radiative transfer model was used to calculate the global erythemally effective irradiance under clear skies. A ratio of the hourly measured to clear-sky modelled irradiance was then derived for zenith angles 35–70°. Subsequent comparisons were then made with routine measurements of sunshine duration at Göteborg and sunshine duration, cloud cover, type and height at Nordkoster.

Cloud transmission of UV-B irradiance decreases with increasing solar zenith angle, with cloud attenuation being 8% stronger at Nordkoster Island for zenith angles >60°. Transmission also decreases with increasing cloud cover such that overcast cloud conditions reduce transmissions by an average of 75%. In addition, cloud type affects the amount of ground incident irradiant flux. *Fractus* cloud afforded the least UV-B transmission (0.16), while *cirrus* filaments afforded the most (0.95).

The spatial and temporal distribution of clouds appears to be non-random. Under conditions of 1 to 3 octas, sky cover, clouds appear to be concentrated in line with the sensor and Sun on more occasions than that expected given a random cloud distribution. The same cloud cover condition also resulted in many instances of ground incident irradiance above clear-sky values. The presence of cumuliform clouds appears to increase the likelihood of the latter phenomena.

1. Introduction

In recent years there has been a substantial increase in attempts to model the radiative flux of biologically effective ultra-violet radiation. However, the incorporation of clouds into the modelling process continues to remain a difficult task due to optical depth and particle density variations in both the spatial and temporal domain.

Previous studies utilising empirical cloud relationships have focused on the broad issues of transmission as a direct function of cloud cover (Ilyas, 1987; Lubin and Fredrick, 1991; Bais et al., 1993; Blumthaler et al., 1996; Nemeth et al., 1996). These results suggests that cloud properties and their spatial distribution can significantly influence the magnitude of the UV irradiance at the Earth's surface.

It is the purpose of this study to examine this topic further by producing detailed estimates of cloud transmission over a time period that both encapsulates the variability in the entire cloud system and provides for results that are statistically valid. The location of interest is Nordkoster Island (58.83° N; 10.72° E), situated in the western Swedish Archipelago for the period 1994 to 1996. Further consideration is also given to sunshine duration at Göteborg (57.69° N; 11.92° E).

2. Data Collection and Processing

The two model 501A UV-Biometers used at both Göteborg and Nordkoster are a continuation of the line of Robertson-Berger broadband detectors. They measure UV-B erythemal irradiance

and display a spectral response with approaches the McKinlay-Diffey erythema action spectrum (1987).

One instrument was deployed on the roof of the Earth Sciences Centre, University of Göteborg, approximately 2 km south-west of the city centre (57.69° N; 11.92° E). It was installed on 21 February 1996 and was running continuously for the duration of this study, with the exception of two periods related to instrument comparison and calibration. Millivolt output from the instrument was fed into a Campbell CR10 data logger at a rate of one data frame every 10 seconds, integrated every 10 minutes and stored on hard disk.

The second instrument was located at Nordkoster Island in the Skagerrak Sea. This site is adjacent to the Norwegian border and is some 7 km and 15 km west of the coast and the town of Strömstad respectively (58.83° N; 10.72° E). Continuous measurements have been conducted since the 2 June 1994 at the research station Kilesandsgarden, Koster health Foundation, University of Göteborg. Signals from the radiometer were also acquired by a Campbell CR10, integrated hourly and stored on hard disk. After 28 May 1996 the signals were integrated every half-hour.

Two field tests were performed on the instruments. The Göteborg instrument was intercompared with another Solar Light 501 Biometer from the Swedish Meteorological and Hydrological Institute (SMHI) which had a calibration traced to a WMO/STUK 1995 intercomparison (Josefsson, 1996 pers. comm.). Comparison of the two instruments (SMHI and Göteborg) at Norrköping (58.58° N; 16.16° E) during a three day period in June 1996 gave a cosine-corrected calibration factor (SMHI/Göteborg) of 1.15 in the zenith angle range 35–55°. All data from the Göteborg instrument was adjusted by this constant factor.

The second comparison was conducted at Nordkoster on the 7th and 8th of May 1996, with the Göteborg and Nordkoster instruments sampling the same ambient irradiance. A linear regression between the two instruments gave:

$$Y = -0.409 + 1.021X(\mathrm{mV})$$

$$r^2 = 0.99$$

where X and Y are the mV output of the Nordkoster and Göteborg instrument respectively. A second field intercomparison was performed at Nordkoster after the field season (12 April 1997). Regression results of 10 minute average comparisons were unchanged from the first intercomparison.

Additional data sources included daily column ozone from Brewer instruments at the WMO stations in Norrköping, Sweden and Oslo, Norway (59.95° N; 10.72° E). Hourly sunshine duration and three hourly cloud type, cover and height were also obtained for Nordkoster. In addition, hourly sunshine duration was obtained for central Göteborg, but cloud data was not recorded there.

This paper uses transmission ratios as the essential statistical unit by which to gauge the behavior of ultra-violet irradiance under clouds. We can define this term by the symbol τ:

$$\tau = UV_c/UV_o$$

where UV_c represents the measured UV-B erythemal irradiance averaged over a time period and UV_o is the clear-sky UV-B erythemal irradiance which would be expected for the same time period and atmospheric constituents.

The radiation data once collected were processed into hourly averages and a clear-sky spectral model was used to calculate cloudless values (Green et al., 1980). A comparison was then made between all measured and modelled data corresponding to clear-sky days at both Nordkoster and Göteborg.

Sunshine duration was used for determining the clear-sky days, however it was noted that very few days existed where the sunshine duration was 100% throughout the whole day. Thus, in order to increase this data set while still maintaining clear-sky validity, it was decided to select hourly data that fell into any period with a minimum of 5 hours of consecutive 100% sunshine duration. Furthermore, if the consecutive sunshine period was less than 7 hours then data corresponding to the first and last hours were deleted. This ensured that the transitional hour between absolute clear-sky and any cloudiness did not influence comparisons. Finally, all the erythemal irradiance data conforming to the sunshine criteria were cross-checked with cloud data and deleted if cloud

cover was greater than 2 octas or less than 5000 metres in height.

The ideal clear-sky data set would produce transmissions approaching unity, thus allowing for a reliable interpretation of the data corresponding to cloudy days. However, daily averages of clear-sky transmission provided ratios between 1.0 and 1.1. Thus it was deemed necessary to provide a correction for this overestimation in order to improve the quality of the transmission data set.

Empirical corrections were thus deemed necessary and calculated as an average of two consecutive clear-sky day transmissions. i.e., the daily ratio of measured to modelled data was calculated for any clear-sky day then averaged with the next clear-sky day transmission. This value was then used as an empirical scaling factor to all cloudy days falling in between. Thus, if τ_i and τ_{i+1} were the two clear-sky daily transmissions, separated by a cloudy period, then the correction factor (C) for the cloudy period is

$$C = (1/\tau_i + 1/\tau_{i+1})/2.0$$

Possible cause for the departure from unity may be sourced to both the modelling and measurement processes. Modelling errors were introduced by the input parameters, especially surface albedo, total column ozone values and aerosol depletion coefficients.

Measurements errors for broadband erythemal radiometers are considerable and an absolute calibration uncertainty of $\pm 10\%$ has been quoted in the literature (Leszczynski et al., 1998). Various factors account for this with the most important being errors in the cosine response, spectral response differences, temperature instability of the sensors and filter deterioration with time (Mayer and Seckmeyer, 1996; Leszczynski et al., 1998). It is not the purpose of this paper to discuss these anomalies. Rather, an empirical correction applied throughout the study is viewed as a means of providing some compensation for this signal error.

Our correction systematically adjusts all data to the Green et al. (1980) model. Therefore, from hereon we utilise only data relative to this 'adjusted' clear-sky value rather than absolute irradiances. It must also be noted that all the clear-sky daily ratios used to adjust the cloudy values were only calculated in the zenith angle range 35–55°. This procedure was deemed to provide a more accurate estimate in accordance with the SMHI comparison listed above.

To ensure compatibility with the three-hourly cloud observations, it was then decided to average all *UV* data falling one hour either side of each cloud observation. This in essence produced a temporally averaged radiation data set compatible with existing cloud data.

The working irradiance data set was finally reduced in order to correspond with zenith angles of 35°–70°, typically experienced during spring, summer and autumn seasons in southern Sweden. This range is larger than the working range for the instrument comparison performed at SMHI (35°–55° zenith). It is possible that larger errors may occur at this higher zenith angle range up to 70°. Examining the data of Mayer and Seckmeyer (1996), a cosine error of 10% may be expected for a zenith angle of 70° and close to 0% at 60°. This translates to a 'mid-range' cosine error of 5%. When considering two data sets, one corresponding to zenith angles less than 60° and the second one between 60° and 70°, the question arises as to the likely differences due to cosine errors. This depends on the diffuse fraction of the irradiance. Assuming isotropy in diffuse radiation and a minimum fraction of 50%, a maximum cosine error of around 3% is obtained. However, it must be kept in mind that the cosine response of Solar Light instruments varies markedly as has been shown in a recent intercomparison paper (Leszczynski et al., 1998) and therefore these results can only serve as a rough guide. This must be kept in mind during the following discussions.

The resultant transmission (measured/cloudless estimate) and total cloud data (octas) remained in data sets corresponding to the individual years 1994–96 before commencement of further analysis. Inter-yearly comparisons at a 10° zenith angle resolution were tested for significance utilising non-parametric statistical measures (Mann-Whitney U test). In order to overcome cloud cover bias, separate tests were performed at 2–3 octas and 6–7 octas (at the 0.05 significance level). Acceptance or rejection of the null hypothesis was only valid if the outcome was the same at both octas bins. If the significance results at each octas bin were contradictory, then the results were deemed inconclusive.

Null hypothesis H_0: *samples X and Y come from populations with the same mean ranks*

Only one of all the possible test combinations deemed that differences were likely to be real. Thus, it was decided to accept the null hypothesis and group all the yearly results into one complete data set.

3. Results and Discussion

3.1 Dependence of Transmission on Zenith Angle

An increase in solar zenith angle provides for a rapid increase in direct radiation path length and associated attenuation by atmospheric constituents. A sensitivity study by Kuchinke (1997) confirmed this, indicating that for a 2° change in zenith angle the attenuation of erythemally effective UV-B irradiance increases from about 5% at 35° to 9% at 70°. The results were obtained under clear-sky and constant ozone conditions at Nordkoster. It was decided to incorporate zenith angle into the cloud modelling process in order to determine if clouds themselves affected irradiance levels as a function of solar zenith angle.

3.1.1 Total Cloud Cover

An average cloud transmission of 70% for Latitude 60° N has been suggested by Fredrick and Snell (1990) and Fredrick and Lubin (1988) from analysis of satellite observations. In addition, *UV* transmission by clouds is estimated to be of the order of 72% in Helsinki and 67% in Saariselka, Finland relative to clear-sky doses. These estimates are based on figures given by Jokela et al. (1993) utilising *UV* distribution maps presented by Josefsson (1986). An approximate calculation for Nordkoster Island based on the same distribution maps indicated an average annual transmission of 71%. In comparison, results from this study suggest an average transmission of 74%. However, it must be noted that data corresponding to winter months were not utilised and as such this may be an overestimate.

For the purposes of comparison throughout the remainder of this study, it was deemed necessary to utilise a normalised mean statistic. An average of the eight median values corresponding to each octa of cloud cover was derived and thus represents an average transmission corresponding to a 'medium' cloud cover scenario. This statistic thus avoids cloud cover bias and was found to be 79% for the entire Nordkoster data set. A comparison of this with the previous result indicates the prevalence of high cloud cover conditions for this region.

Several representations of transmission versus total cloud cover have been presented in the literature and are based on a linear fit with the data of the form:

$$UV_c/UV_o = 1 - Fc$$

where UV_c and UV_o are cloudy and clear skies respectively, c is fractional cloud coverage and F an extinction coefficient due to cloud attenuation. Values of 0.56 (Green et al., 1974; Ilyas, 1987) and 0.50 (Cutchis 1980) have been quoted for F. Furthermore, Josefsson (1986) presents a power regression of the form $1–0.7c^{2.5}$ for measurements conducted at Norrköping, inland Sweden.

Results from Nordkoster 1994–1996 indicate quadratic fits to the data (Fig. 1 and below). One explanation for the apparent differences in form is the time scale of data measurements. Much published data corresponding to the linear fits were at a daily or monthly time scale as opposed to hourly. This tends to have a moderating affect

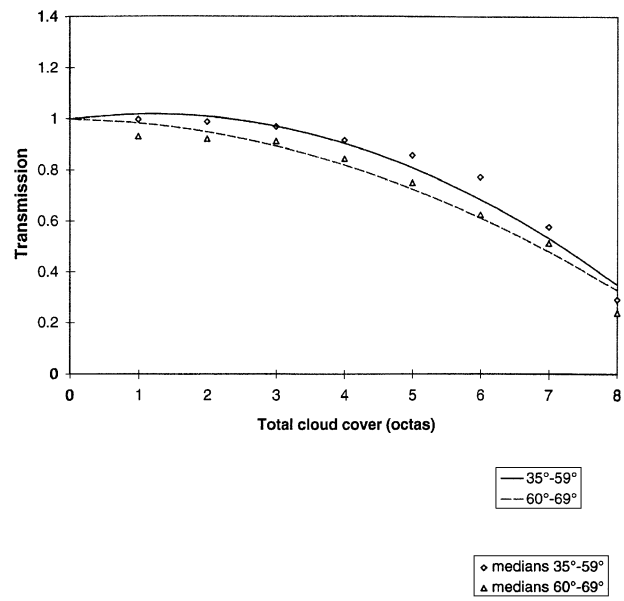

Fig. 1. UV-B transmission vs total cloud cover

on the data and will consequently reduce regression complexity (cf. section 3.3.2). Implicit in the quadratic form is the fact that other parameters such as cloud optical thickness are evolving with cloud cover and thus affecting the relationship.

Results from Figure 1:

$$UV_c/UV_o = 1 + 0.0266c - 0.0132c^2 \quad \text{for } \theta_z = 35°\text{–}59°$$
$$= 1 + 0.0065c - 0.0097c^2 \quad \text{for } \theta_z = 60°\text{–}69°$$
$$c = \text{octas cloud cover}$$

The regressions here correspond to all the data and were forced to a transmission of 1.0 for conditions of no apparent cloud cover. In addition, median values corresponding to each octa of total cloud cover were calculated for each zenith bin and are also presented in Fig. 1.

Significance tests at 2–3 octas and 6–7 octas for 10° zenith bins 35–39°, 40–49° and 50–59° indicated the null hypothesis to be true and thus differences in transmission were only due to chance. However, a comparison of these bins with data corresponding to zenith angles 60–69° rejected the null hypothesis in all instances. Thus, differences between this high zenith angle bin and the others appeared to be as a result of a true fluctuation in transmission, independent of differences in cloud cover distribution.

In addition, ratios in the 60–69° zenith angle bin were lower for all cloud cover data. Percent differences in median transmission between the two bins ranged from a minimum of 5.3 to a maximum of 14.7. These differences appear too large to be purely a result of instrument cosine errors. Furthermore, the lower ratios are maintained for high cloud cover conditions when very little direct radiation is expected (and therefore very little difference between the two data sets due to cosine errors).

The derived regression corresponding to zenith angles 35–59° produced a coefficient of determination (r^2) of 0.80 from a population of 622 samples. The 60–69° zenith bin produced a lower coefficient of 0.76 from 168 samples. Similar quadratic expressions were obtained by Lubin and Fredrick (1991) for measurements over Antarctica and Nunez et al. (1994) at Hobart, Australia. However, fits to the Nordkoster data suggest much stronger attenuation by clouds for conditions of high cloud cover. This implies that optically thicker clouds may be correlated with larger cloud coverage at Nordkoster.

Additional statistical data for the zenith bins 35–59° and 60–69° indicates that transmission is reduced and there is a wider scatter for the higher zenith bin. The lower bin is characterised by an interquartile range of 0.77 to 1.01 and mean of 0.80. In comparison, the higher zenith angle bin has corresponding statistics of 0.43 to 0.83 and mean of 0.72. Thus, it must be noted that intra-zenith bin comparisons of these statistics indicate a sample bias towards higher transmissions at lower zenith angles and lower transmissions at higher zenith angles.

3.1.2 Zenith Angle Dependency for Different Cloud Altitudes

Transmission data were grouped according to low (< 2500 metres), medium (2500–5000 metres) and high cloud base (> 5000 metres). However, the number of medium and high cloud base records were low due to the sampling method. Thus, it was decided to classify cloud level data into coarse zenith angle bins of 35–52° and 53–69°. The corresponding significance tests at 2 to 3 octas and 6 to 7 octas indicated that at this zenith angle resolution, real zenith angle dependency was only evident for low clouds i.e., cloud base less than 2500 metres. For clouds above this level, differences were deemed to be as a result of chance fluctuations between 2500 and 5000 metres and inconclusive for heights greater than this, possibly due to low sample numbers.

Figure 2a depicts transmission data corresponding to low cloud. Results corresponding to higher zenith angles indicate lower median transmissions at all octas. Consideration must be given to the fact that the low cloud data accounts for nearly 80% of the total cloud data set. Since the majority of clouds above 2500 metres display no significant transmission $\sim$ zenith angle dependency, it must be concluded that low cloud is largely responsible for the zenith angle phenomena observed by the total cloud data (Fig. 1).

3.2 Dependence of Transmission on Cloud Height

3.2.1 Discrete Levels

Data corresponding to distinct cloud levels was classified on the basis of height and zenith angle as indicated in section 1.2. Transmission results between levels were compared to see if any observed differences at 2–3 and 6–7 octas were significant or not. Interestingly enough, significance for both octa bins only occurred between data corresponding to low and high cloud. In other instances, the differences were simply due to random fluctuations in transmission or were inconclusive.

Borkowski et al. (1977) first suggested in 1975 that high clouds have much less effect on the sky ultraviolet radiation arriving at the ground. Results here produced significantly different low cloud mean transmissions of 0.74 (35–52°) and 0.66 (53–69°), a medium cloud transmission of 0.83 and high cloud overall transmission of 0.93. Thus, the differences become apparent and are of the order of 20 to 25% from high to low cloud.

A graphical representation of individual results confirms this and shows that, given an increase in cloud level, surface UV-B levels are less affected by an increase in cloud cover (Fig. 2a–c). Low clouds such as *stratus* and associated forms appear to transmit UV-B similarly to results obtained for total cloud data. However, medium clouds (*alto* genera) and high clouds (*cirrus* genera) display a more linear transmission trend. High clouds of the genera *cirrus*, *cirrocumulus* and *cirrostratus*, when present, have relatively no effect on UV-B for partial cloud cover and transmit 82% of UV-B for extensive cloud cover, corresponding to the 25th percentile obtained under 7 octas conditions (there were no instances of medium or high cloud cover corresponding to 8 octas).

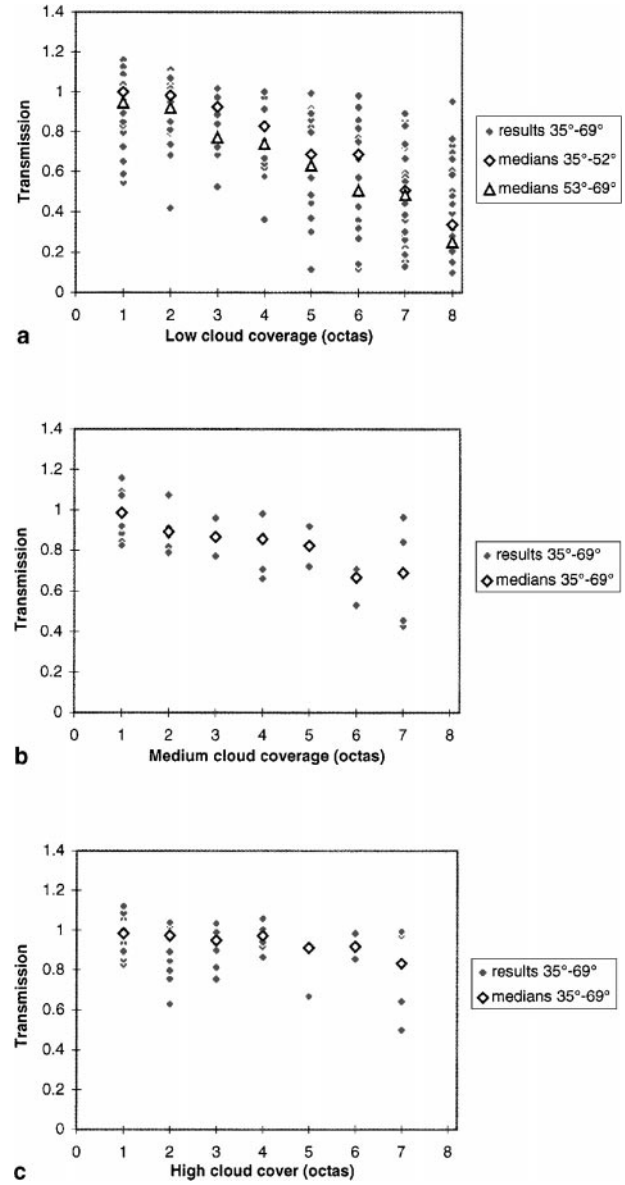

Fig. 2. a) UV-B transmission vs low cloud cover. b) UV-B transmission vs medium cloud cover. c) UV-B transmission vs high cloud cover

3.2.2 Cloud Type

Implicit to the notion of cloud height dependency is the actual form a particular cloud resembles. Clouds themselves are classified by genera where part or all of the assigned title affixes the cloud to an approximate height interval. It has been indicated in the literature that cloud type may be a poor parameter to consider due to the variety of forms that can be inherently represented by any one cloud (Fredrick and Steele, 1995; Estupiñán et al., 1996). It must be added that cloud height may also vary for a particular cloud type. This in itself has important repercussions for the effect of aerosols and other atmospheric attenuators that exist in the spatial cloud domain. Thus one needs to exercise caution when modelling cloud type directly. However, the cloud type data acquired from SMHI was deemed to be at

Table 1. *UV-B Transmission for Significant Cloud Types*

Cloud type	UV-B Transmission
Stratus	0.79
Stratocumulus	0.62
pannus (stratus fractus/cumulus fractus)	0.16
altostratus	0.39*
altocumulus (single opaque layer)	0.70
–"– (multiple opaque layers)	0.72
–"– (high invading towers)	0.78
cirrus (sparsely distributed filaments)	0.97
–"– (invading filaments)	0.95
cirrostratus (unobtrusive)	0.94
cirrostratus (entire celestial dome)	0.85

*inconclusive result

least as accurate as the coverage data, prompting its inclusion for the purposes of comparison.

Transmissions for each cloud type were derived and are shown in Table 1. As with previous data, statistics for each cloud type were initially grouped into octa categories and for each of these categories the median value was determined. The final step was to average all the median values provided there were at least 5 data values in each octa bin. Therefore the results in Table 1, with the exception of *pannus* and *altostratus*, may again be interpreted as a mean transmission for 'medium' cloud cover.

In the case of low cloud *pannus* (*stratus fractus* and *cumulus fractus*), results indicate that this cloud type transmits UV-B levels the least, with transmission of the order of 16%. They are generally associated with bad weather in the form of rain or showers and it was noted that all 46 instances of this cloud type corresponded with completely overcast conditions. With this in mind, attenuation was still the strongest under these conditions compared to all other cloud types.

Medium level clouds of the genera *altostratus* also displayed low transmission ($\tau = 0.39$) and again were only present during fully overcast conditions. However, the resultant transmission was not significantly low compared to other cloud types at 8 octas. In addition, they often represented the form *nimbostratus*, whose base lies well below 2500 metres. Thus, in this instance the results were deemed inconclusive.

Other strong attenuators are clouds of the type *stratocumulus* ($\tau = 0.62$), *altocumulus* (single opaque layer, $\tau = 0.70$, multiple opaque layers, $\tau = 0.72$, high invading towers, $\tau = 0.78$) and *stratus* ($\tau = 0.79$). The recorded low level *stratocumulus* had not evolved from *cumulus* cloud and the low level *stratus* was present in a more or less continuous sheet or layer. The aforementioned cloud types all appeared to be evenly distributed with cloud cover and results suggest that an increase in thickness of *altocumulus* cloud (2500 to 5000 metres) enhances ground incident UV-B irradiance, possibly due to increased forward scattering.

Clouds which affect incoming UV-B the least appeared to be of the genera *cirrus*. Under all conditions of cloud cover, when *cirrus* filaments invaded the sky the average transmission was of the order of 95% and was increased to 97% when filaments were more sparsely distributed. *Cirrostratus* cloud produced an average transmission of 94%, however this was only evident when the form for this particular type was not particularly obtrusive across the sky. If the extent of this cloud breached the entire celestial dome, transmission was of the order of 85%.

To summarise, Tsay and Stamnes (1992) came to the conclusion that *stratus* clouds provide significant protection from UV-B exposure, based on low transmission values recorded during Arctic summertime. Results here suggest that other cloud types provide similar transmissions, with the lowest values generally afforded by low *fractus* clouds. However, it must be stressed that the derived transmissions are only averages based on estimates of cloud cover. At any one time the cloud field is constantly moving and fluctuations over the period of several hours may produce transmissions that are significantly different from those given in Table 1.

3.2.3 Cloud Base Height

The effects of cloud height independent of cloud type are illustrated in Fig. 3. Here, cloud height was estimated to the nearest 30 metres for cloud base less than 1500 metres, and to the nearest 300 metres for cloud base height between 3000 and 9000 metres. Samples were once again biased for low altitude cloud due to the sampling method. In addition, it was not possible to provide accurate graphical representations of height trends at each octa. Considerable overlap

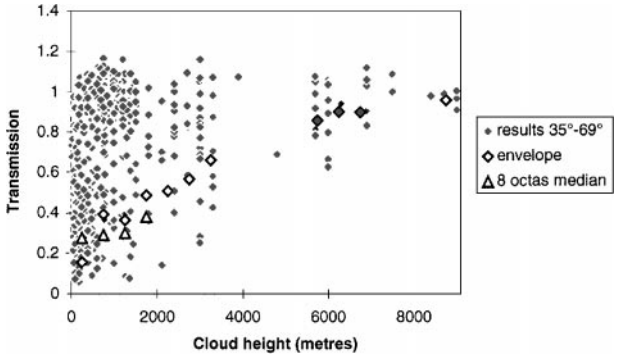

Fig. 3. UV-B transmission vs cloud height

was evidenced in the 3–6 octas range due to the low number of recordings at high altitude and variation in optical cloud thickness at low altitude. Thus, the large scatter is an artifact of the representation of recordings at all octas of cloud cover.

In order to discern trends, transmissions were grouped at cloud height intervals of 500 metres. Median values corresponding to fully overcast conditions were subsequently calculated and were found to approximate the 10th percentile where sample numbers permit (Fig. 3). The resultant percentile statistic is thus an envelope predicting the minimum transmission that is likely to occur under overcast cloud conditions at each altitude level. The form of the overcast envelope itself appears to be non-linear and again indicates more rapid attenuation change at low altitudes.

3.3 Spatial/Temporal Trends

It became clear during the modelling process that clouds display high variability both spatially and temporally. Analysis so far has acknowledged the existence of such trends through the choice of modelling steps taken in order to encapsulate this variability and avoid bias. However, a more comprehensive investigation of both the spatial and temporal cloud distribution patterns was deemed relevant and important.

3.3.1 Dependence of Transmission on Sunshine Duration

Plots of the ratio UV_c/UV_o erythemal UV-B irradiance versus sunshine duration were constructed from the data for 1994 to 1996 at Nordkoster and 1996 at Göteborg, some 200 km to the south. The regression corresponding to sunshine duration at Göteborg provided an r^2 value of 0.65, whereas the Nordkoster data produced a lower coefficient of 0.56. It was noted that data corresponding to Nordkoster were only estimated to the nearest 10 percent and thus may be less reliable. However, due to the large number of recordings, the regressions obtained at both sites were deemed suitable for comparison (Fig. 4a and b).

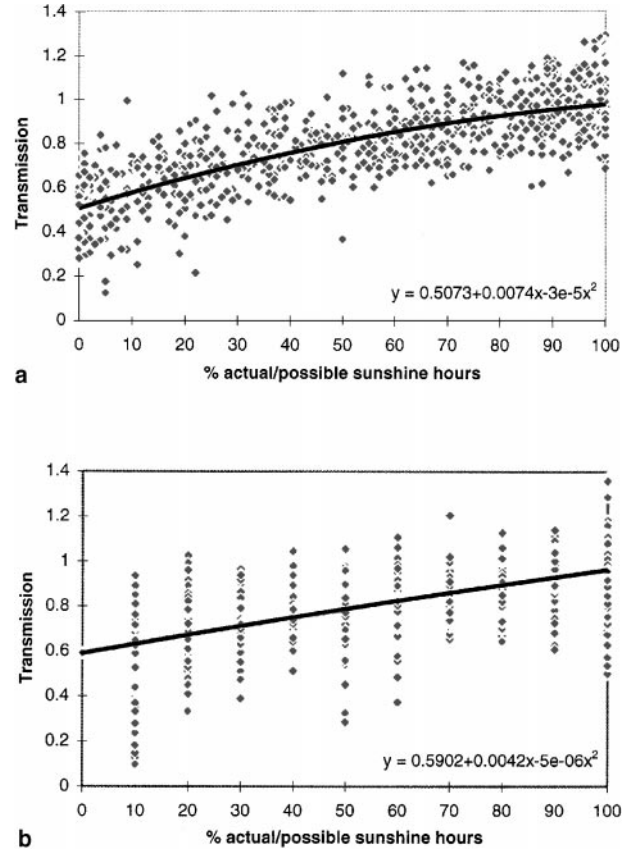

Fig. 4. a) UV-B transmission vs sunshine duration at Göteborg, 1996 for zenith angles 35° to 69°. b) UV-B transmission vs sunshine duration at Nordkoster, 1994–1996 for zenith angles 35° to 69°

The results showed that transmission is 10% higher at Nordkoster for periods of low sunshine duration, whereas maximum sunshine results in a convergence of data sets such that they are almost equal. Implicit in sunshine duration is the concept of spatial/temporal averaging, such that if the direct sunshine at any two locations over the same time period is equal, then the temporal

distribution of cloud cover is also equal. Thus, for moderate to overcast cloud conditions, cloud parameters such as thickness and altitude are responsible for differences between the two data sets.

In addition, the results display the effect clouds have on the ratio of direct to diffuse irradiance. At 100% sunshine duration, transmission approximates 1.0, whereas a reduction in bright sunshine does not accord with a linear decrease in transmission to zero for low sunshine. This is due to the strong scattering of UV-B under high cloud conditions such that the ratio of diffuse to direct is increased. Thus, periods of zero percent sunshine duration are analogous to overcast conditions, where the direct radiation is totally depleted and only diffuse radiation predominates at the surface.

3.3.2 Time Averaged Analysis

By deriving a ratio of average UV_c/average UV_o for different time periods, we attain results which may be more significant i.e., they may be deemed to be more 'climatologically useful' when trends are expressed over greater time intervals. In doing so, we inadvertently apply a 'smoothing' filter to the data where fluctuations are damped out by the averaging process.

Cloud transmissions were calculated for Nordkoster and compared with average percent sunshine duration and average total cloud cover at the daily, weekly and monthly time scales. Statistics given in Table 2 indicate the expected improvement in standard deviation for increase in time scale. In addition, the calculated mean values indicate certain trends. The mean value again represents the average of the median values obtained at each 10% interval of sunshine duration or octa of total cloud cover, thus avoiding sample bias. The results clearly show that the sunshine data were biased towards hours of high duration, as given by the increase in the mean for greater time scales. In contrast, the total cloud cover mean remains relatively constant at all time scales and as such this data were deemed to be equally represented at all octa levels.

Table 2. *Time Scale Variation on Transmission vs total Cloud Cover and Sunshine Duration*

Data set	Time scale	n	mean	SD
Sunshine	hourly	3429	0.81	0.18
duration	daily	430	0.90	0.15
(%)	weekly	70	0.92	0.11
	monthly	19	0.93	0.09
Total cloud	hourly	790	0.79	0.25
cover	daily	487	0.80	0.24
(octas)	weekly	73	0.79	0.17
	monthly	19	0.80	0.12

Plots of the weekly and monthly figures are given in Fig. 5a–d. Results confirm that sunshine data is biased towards higher values, with monthly figures congregating between values of 70 and 90% of hourly bright sunshine. This pattern is further evidence of the much higher frequency of high sunshine duration events compared to low sunshine duration events. For example, hourly data statistics from Fig. 4b gave 2341 occasions in the range 90–100% actual/possible sunshine hours as opposed to 416 occasions in the 10–20% range. In contrast, the total cloud cover appears to be more evenly represented at all octas by the weekly data and converges towards 2 to 6 octas cover at the monthly scale. Over this period, only a slight bias is noticeable, as more months are characterised by average cloud cover of 5–6 octas.

With respect to the monthly transmission data (Fig. 5b and 5d), two months (August and September 1996) appear as outliers from the apparent trend and are highlighted (right to left) in both graphs. The cause for this is not immediately apparent. Correction factors taken for clear-sky days would normalise data for a range of atmospheric constituents. However, these two months were characterised by coastal haze (Nunez and Chen, 1997) and it is possible that a correction factor that was derived for cloudless conditions may not adequately represent the larger path length and depletion expected with diffuse cloudy conditions.

3.3.3 Cloud Distribution Patterns

Of particular interest to this study is the occurrence of cloud transmission values that are greater than normal clear-sky levels. This phenomena has been widely reported in the literature (Nack and Green, 1974; McCormick and Suehrcke, 1990; Segal and Davis, 1992) with increases ranging from 4 to 25% above clear-sky levels (Bais et al., 1993; Mims and Fredrick,

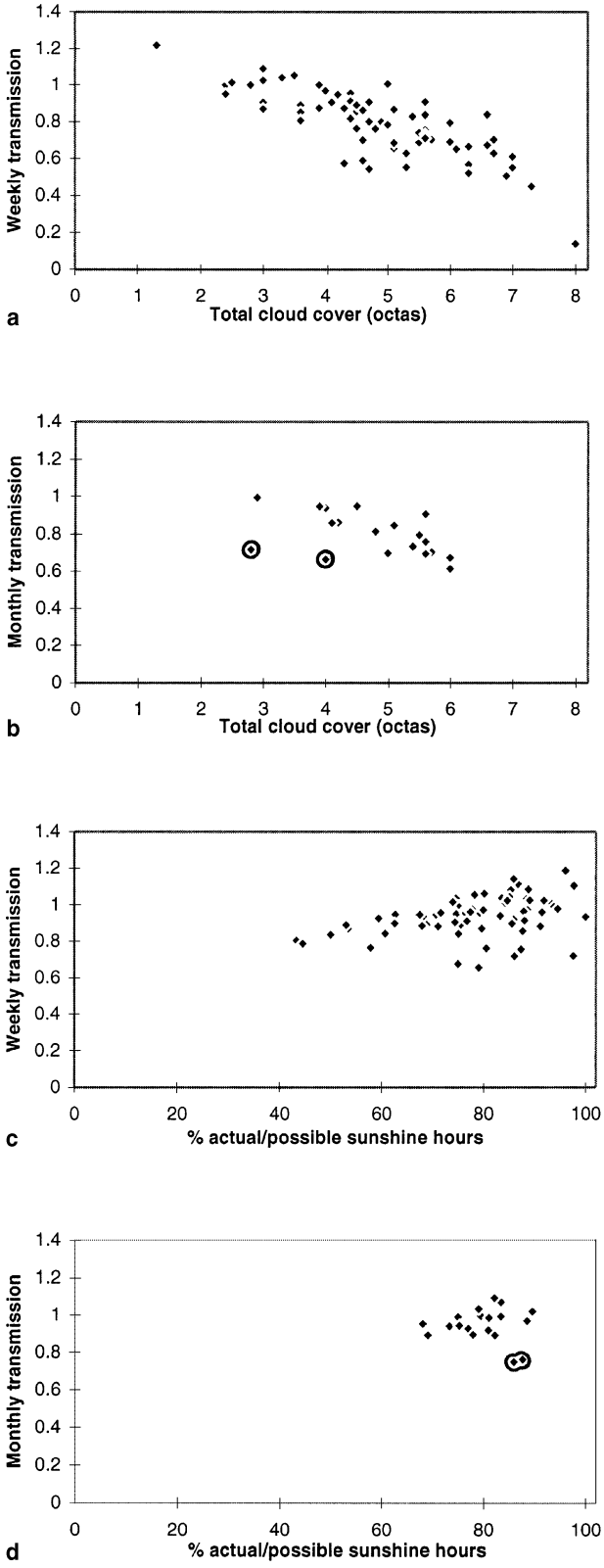

Fig. 5. a) Weekly UV-B transmission vs total cloud cover, Nordkoster 1996. b) Monthly UV-B transmission vs total cloud cover, Nordkoster 1996. c) Weekly UV-B transmission vs sunshine duration, Nordkoster 1996. d) Monthly UV-B transmission vs sunshine duration, Nordkoster 1996

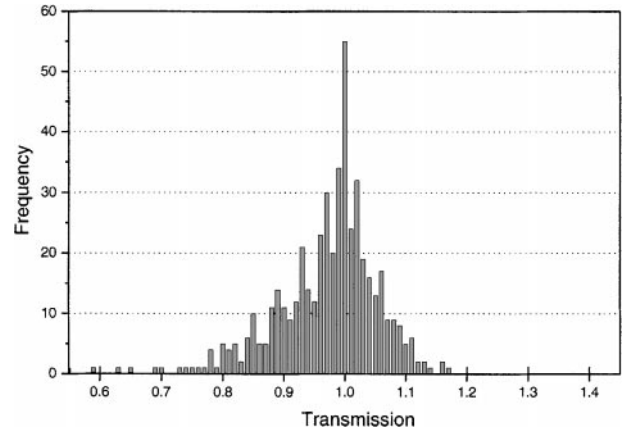

Fig. 6. UV-B cloud transmission frequencies, 1 to 3 octas cloud cover

1994). Results imply that clouds may actually increase surface incident irradiance under certain conditions. In all reported instances partial cloud conditions were responsible, as was the case at Nordkoster (Fig. 2a–c) where much of the data reported high values at 1–3 octas cloud cover.

However, little attention has been focused on the spatial distribution of clouds and its possible effect on surface incident irradiance. If clouds were randomly distributed at the spatial scale, then a sufficient sample size at 1–3 octas cloud coverage would result in transmissions less than 1.0 on ~25% of occasions. Figure 6 depicts a frequency distribution of all transmissions at Nordkoster occurring at 1–3 octas total. Results suggest that at this sky coverage the cloud spatial distribution is predisposed to transmissions less than 1.0 on 60% of occasions and is thus non-random.

Further insight can be obtained by referring to daily averages of percentage sunshine and total cloud cover contained in Table 3. The percentage of bright sunshine in column 2 corresponds to a random sky distribution of clouds between the Sun and the sensor for each octa value. Measured data indicates that at cloud cover of 2–3 octas there is less daily sunshine arriving at the sensor than expected given a random cloud distribution. This implies that the temporal distribution of clouds is non-random and increased at this cloud coverage. The converse was true for days of high cloud cover where the daily sunshine was much higher than expected for random cloud patterns. This anomaly appears to be an artifact of the error associated with overestimation of cloud

Table 3. *Daily Sunshine Duration vs Total Cloud Statistics*

Daily octas	% Sunshine duration given random cloud distribution	Measured daily sunshine duration	Difference
1	87.5	97.1	9.5
2	75.0	71.2	−3.8
3	62.5	57.5	−4.0
4	50.0	54.0	4.0
5	37.5	56.1	10.6
6	25.0	49.0	24.0
7	12.5	29.2	16.7
8	0	34.0	34.0

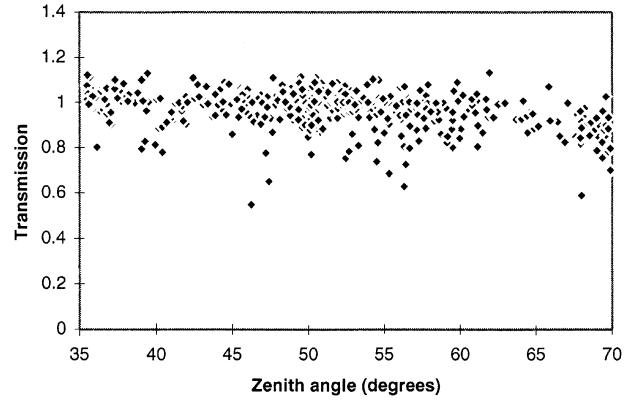

Fig. 7. UV-B transmission vs zenith angle, 1–3 octas cloud cover

cover. When clouds invade the sky, the observer may inadvertently express the cloud height domain as a component of the horizontal coverage, a quantity which may differ from the recorded sunshine duration. Sunshine data at 1 octa displayed a similar pattern, however results appear to have been confounded by many instances of 100% sunshine and were thus approximating clear-skies.

In retrospect, it appears that there exists differences in the spatial distribution of low cloud cover above Nordkoster Island. The entire data set spans the period early spring to mid autumn and it is during this period that westerly flow dominates and sea-breeze days are frequent, averaging 5 to 6 ms^{-1} (Gustavsson et al., 1995). According to Oke (1987) a common sea-breeze of 2 to 5 ms^{-1} extends inland for 1 to 2 km and affects the airflow up to 2000 metres. During days of this description, clouds returning to sea by upper air counterflow may not have dissipated over Nordkoster. Rather, an accumulation of scattered cloud may occur in a specific region of the sky.

3.3.4 Enhanced Irradiance Levels

The occurrences of transmissions greater than 1.0 in Fig. 6 appear to be a consequence of the accumulation of the direct beam and cloud side reflections at the point source. A suggestion has been made that for solar angles close to the zenith, *cumulus* clouds can significantly increase UV-B levels (Mims and Fredrick, 1994).

In this study, a comparison between UV-B transmission and zenith angle was undertaken corresponding to 1–3 octas total cloud cover (Fig. 7). Site latitude restricts the comparison to zenith angles greater than 35°, however a trend was still evident. The results show that UV-B transmission at 1–3 octas displays only slight zenith angle dependence between 35° and 60°, although some change is noticeable for higher zenith angles (Fig. 7). This reinforces the fact that spatial processes are dominant. It does not appear that higher zenith angles in the range 35–70° provide for much UV-B enhancement. Rather it is the pattern of spatial cloud distribution that determines this.

Side reflection as a phenomena appears to be more prevalent for low cloud conditions. A total of 411 samples containing significant frequencies for specific cloud types were grouped and presented in Table 4. The results suggest that low cumuliform clouds are equally as likely to

Table 4. *Cloud Type Frequency of Occurrence, 1 to 3 Octas Total Cloud Cover*

Cloud type	Frequency	
	$\tau < 1.0$	$\tau > 1.0$
cumulus (little vertical extent – good weather)	36	44
cumulus (strong vertical extent)	53	49
stratocumulus (formed from cumulus)	5	15
stratus (continuous sheet)	14	8
altocumulus (semitransparent single level)	14	3
altocumulus (towers invading the sky)	14	–
cirrus (filaments not invading the sky)	79	28
cirrus (tufts)	14	18
cirrus (bands to horizon, invading the sky)	14	3

result in transmissions above or below clear-sky values. However, they do account for almost 70% of enhanced UV-B recordings. This finding accords with results by Mims and Fredrick (1994) and Estupiñán et al. (1996). Cloud thickness is thus an important parameter here, increasing the chances of multiple side reflection and agglomeration at the sensor.

4. Summary and Conclusions

It was the objective of this study to estimate cloud transmission of UV-B erythemal irradiance at Nordkoster Island and assess any resultant trends in the data. In order to achieve this objective, ground based measurements of erythemal UV-B irradiance were collected over a three year period 1994 to 1996. A subsequent analysis with cloud and sunshine data established the following relationships applicable to the Nordkoster cloud field.

1. Results indicate that the average cloud attenuation of UV-B from its cloudless value is 26%. Measurements correspond to medium cloud cover conditions for the seasons of spring, summer and autumn and zenith angles of 35–70° (35° approximates noon of the summer solstice). Overcast cloud conditions at Nordkoster produce an average UV-B transmission of 25%.
2. An increasing solar zenith angle will relate to an increasing ray-path length. It is thus noted that high zenith angles give high ratios of diffuse to direct radiation as a result of increased scattering by ozone, aerosols and molecules. Results at Nordkoster indicate that cloud attenuation is on average 8% stronger for all data corresponding to zenith angles $>60°$, implying a marked reduction in forward scattering at these angles. The phenomena is more noticeable under partial cloud conditions and may be attributed to a combination of increased back reflection of the direct beam and the fact that much radiation is already in the diffuse form.
3. Transmission is least for cloud types with bases below 2500 metres altitude, with average transmission being 70%. At these altitudes, clouds of the genera *fractus* displayed greatest optical thickness and were equivalent to overcast conditions ($\tau = 16\%$). Low *stratocumulus* clouds displayed an average transmission of 62%, however under conditions of 1–3 octas sky cover they may actually increase doses above clear-sky values. Clouds between 2500 and 5000 metres displayed an average transmission of 83%. *Altocumulus* clouds displayed the lowest average transmission in this range (70%), but only when present as a single opaque layer. A relative increase in thickness of this cloud type increased ground UV-B levels. Clouds above 5000 metres transmitted UV-B irradiance by 93% on average, with *cirrostratus* clouds having the lowest transmissions here. All results correspond to a normalised 'medium' cloud cover scenario.
4. Time averaged data indicate relatively unbiased total cloud cover recordings throughout the course of this study. In contrast, much sunshine data tended towards hours of high sunshine duration. Specific clusters were evident in all monthly averaged data except August and September 1996. Here, aerosols in the form of coastal haze may be influencing the results. The GCS clear-sky model and associated correction factors simulate atmospheric attenuation to a certain degree of accuracy. However, if atmospheric aerosols increase, the adopted modelling procedure may fail to compensate for this when clouds are present. A combination of clouds and high aerosols loadings may amplify UV attenuation for the two anomalous months.
5. The spatial and temporal distribution of clouds at Nordkoster Island appears to be non-random. Under conditions of 1–3 eighths sky cover, clouds appear to block the direct beam on more occasions than expected given a random cloud distribution. Synoptic conditions as a result of the maritime environment may be the cause. For a more accurate determination of this phenomena, analysis of time series digital images from a fish-eye lens is recommended.
6. Many instances of surface UV-B dose above a clear-sky value were recorded and in agreement with published literature we believe that side reflection from clouds is the likely explanation. The pattern appears to be zenith angle independent, but cloud thickness is important.
7. The pattern of spatial distribution of cumuliform clouds is relevant to and influential on

the radiation field. Their presence appears to increase the likelihood of enhanced ground UV-B doses but only under conditions of partial cloud cover. During these occasions the net result is high if the transmission process focuses irradiance flux towards the sensor, as opposed to a more homogeneous scattering. Thus, cloud edges may be acting as lenses, increasing levels of damaging UV-B at the ground.

Acknowledgements

The authors would like to acknowledge Deliang Chen for his invaluable assistance at the Earth Sciences Centre, University of Göteborg, Sweden. Thanks is also extended to the Swedish Meteorological and Hydrological Institute (SMHI) for the cloud and sunshine data and to Weine Josefsson (SMHI) for assistance with UV Biometer calibration. This research was funded by the Swedish Radiation Protection Institute.

References

Bais, A. F., Zerefos, C. S., Meleti, C., Ziomas, I. C., Tourpali, K., 1993: Spectral measurements of solar UVB radiation and its relations to total ozone, SO_2, and clouds. *J. Geophys. Res.,* **98** (D3), 5199–5204.

Blumthaler, M., Ambach, W., Cede, A., Staehelin, J., 1996: Attenuation of erythemal effective irradiance by cloudiness at low and high altitude in the alpine region. *Photochemistry and Photobiology,* **63** (2), 193–196.

Borkowski, J., Chai, A., Mo, T., Green, A., 1977: Cloud effects on middle ultraviolet global radiation. *Acta Geophysica Polonica,* **25** (4), 287–301.

Cutchis, P., 1980: A formula for comparing annual damaging ultraviolet (DUV) radiation doses at tropical and mid-latitudes sites. Federal Aviation Administration Report FAA-EE 80–21, Washington D. C.

Estupiñán, J. G., Raman, S., Crescenti, G. H., Streicher, J. J., Barnard, W. F., 1996: Effects of clouds and haze on UV-B radiation. *J. Geophys. Res. Atmospheres,* **101** (D11), 16807–16816.

Fredrick, J. E., Lubin, D., 1988: The budget of biologically active ultraviolet radiation in the earth-atmosphere system. *J. Geophys. Res.,* **93** (D4), 3825–3832.

Fredrick, J. E., Snell, H. E., 1990: Tropospheric influence of solar ultraviolet radiation: the role of clouds. *J. Climatol.,* **3** (3), 373–381.

Fredrick, J. E., Steele, H. D., 1995: The transmission of sunlight through cloudy skies: an analysis based on standard meterological information. *J. Appl. Meteor.,* **34**, 2755–2761.

Green, A. E. S., Mo. T., Miller, J. H., 1974: A study of solar erythema radiation doses. *Photochemistry and Photobiology,* **20**, 473.

Green, A. E. S., Cross, K. R., Smith, L. A., 1980: Improved analytic characterization of ultraviolet skylight. *Photochemistry and Photobiology,* **31**, 59–65.

Gustavsson, T., Lindqvist, S., Borne, K., Bogren, J., 1995: A study of sea and land breezes in an archipelago on the west coast of Sweden. *Int. J. Climatol.,* **15**, 785–800.

Ilyas, M., 1987: Effect of cloudiness on solar radiation reaching the surface. *Atmos. Environ.,* **17**, 2069–2073.

Jokela, K., Leszczynski, K., Visuri, R., 1993: Effects of Arctic ozone depletion and snow on UV exposure in Finland. *Photochemistry and Photobiology,* **58** (4), 559–566.

Josefsson, W., 1986: Solar ultraviolet radiation in Sweden. SMHI report 53, National Institute of Radiation Protection in Stockholm, Norrköping, Sweden.

Kuchinke, C., 1997: Sensitivity study-UV-B irradiance: Project work on Modelling Report Series B (published), Earth Sciences Centre, University of Göteborg, pp. 31–38.

Leszczynski, K., Jokela, K., Yllanttila, L., Visuri, R., Blumthaler, M., 1998: Erythemally weighted radiometers in solar UV monitoring: Results from the WMO/STUK intercomparison. *Photochemistry and Photobiology,* **67** (2), 212–221.

Lubin, D., Fredrick, J. E., 1991: The ultraviolet radiation environment of the Antarctic peninsula: the roles of ozone and cloud cover. *J. Appl. Meteor.,* **30**, 478–493.

Mayer, B., Seckmeyer, G., 1996: All-weather comparison between spectral and broadband (Robertson-Berger) UV measurements. *Photochemistry and Photobiology,* **64** (5), 792–799.

McKinlay, A. F., Diffey, B. L., 1987: A reference action spectrum for ultraviolet induced erythema in human skin. *CIE Journal,* **6** (1), 17–22.

McCormick, P. G., Suehrcke, H., 1990: Cloud-reflected radiation. *Nature,* **345**, 773.

Mims, F. M., Fredrick, J. E., 1994: Cumulus clouds and UV-B. *Nature,* **371**, 291.

Nack, M. L., Green, A. E. S., 1974: Influence of clouds, haze and smog on the middle ultraviolet reaching the ground. *Appl. Opt.,* **13** (10), 2405–2415.

Nemeth, P., Toth, Z., Nagy, Z., 1996: Effect of weather conditions on UV-B radiation reaching the earth's surface. *J. Photochemistry and Photobiology,* **32** (3), 177–181.

Nunez, M., Chen, D., 1998: A comparison of cloudless sky erythemal ultraviolet radiation at two sites in southwest Sweden. *Int. J. Climatol.,* **18**, 915–930.

Nunez, M., Forgan, B., Roy, C., 1994: Estimating ultraviolet radiation at the earth's surface. *Int. J. Biometeorology,* **38**, 5–17.

Oke, T. R., 1987: *Boundary Layer Climates,* 2nd ed. London: Routledge.

Segal, M., Davis, J., 1992: The impact of deep cumulus reflection on the ground-level global irradiance. *J. Appl. Meteor.,* **31** (2), 217–222.

Tsay, S. C., Stamnes, K., 1992: Ultraviolet radiation in the Arctic: the impact of potential ozone depletions and cloud effects. *J. Geophys. Res.,* **97**, 7829–7840.

Authors' address: Christopher P. Kuchinke (kuchinke@postoffice.utas.edu.au) and Manuel Nunez, School of Geography & Environmental Studies, GPO Box 252-78, Sandy Bay, Tasmania, Australia 7001.